Proc. Natl. Acad. Sci. USA
Vol. 90, pp. 8643–8647, September 1993
Medical Sciences

Microphotocoagulation: Selective effects of repetitive short laser pulses

JOHANN ROIDER*†‡, FRANZ HILLENKAMP*§, THOMAS FLOTTE*, AND REGINALD BIRNGRUBER*¶

*Wellman Laboratories of Photomedicine, Harvard Medical School, Massachusetts General Hospital, Boston, MA 02114; §Institute for Medical Physics and Biophysics, University of Münster, 48149 Münster, Germany; ¶Medical Laser Center GmbH, 23562 Lübeck, Germany; and †Medical University of Lübeck, Klinik für Augenheilkunde, Ratzeburger Allee 160, 23538 Lübeck, Germany

Communicated by Erich P. Ippen, January 19, 1993

ABSTRACT **Repetitive exposure to short laser pulses is shown to cause selective damage to absorbing structures (cells, organelles, or enzymes) with pulse energies below the threshold energy for single-pulse damage. Directly adjacent structures are spared *in vivo*. Additivity of (presumably nonphotochemical) subthreshold effects is demonstrated. Selective damage to the retinal pigment epithelium with sparing of the neural retina is shown (514 nm, 5 μs, 1–500 pulses at 500 Hz, 2- to 10-μJ pulse energy). A melanin granule model has been developed and applied to the experimental situation. Histological results as well as the basic mechanism for these effects are discussed.**

Depending on the type of tissue and the wavelength used, laser light can be absorbed by uniformly distributed chromophores and water or by discrete pigment granules. For many applications, laser light energy is transformed into inner energy (heat) of the absorbing structures. Thermal effects prevail at exposure times > 1 ms (1, 2). Depending on the exposure time, these effects may not be confined to the absorbing structures. During and after exposure, heat dissipates out of the absorbing volume, causing a substantial temperature increase in the surrounding tissue and undesirable side effects. In clinical retinal photocoagulation, for example, with exposure times of several hundred milliseconds, the nonabsorbing neural retina is thermally damaged because it is directly adjacent to the absorbing retinal pigment epithelium (RPE). However, in several diseases only the destruction of the RPE, a single cell layer, is required (3–5).

Such confined effects require the use of pulses shorter than the thermal relaxation time of the target structure (adiabatic heating) (6). Thermal effects are temperature- and time-dependent and highly nonlinear (1, 6–8). As the exposure time and therefore the time of increased temperature becomes shorter, higher temperatures are necessary to achieve a given effect. If the energy is deposited in a very short time (typically microseconds or less), large spatial and temporal temperature gradients result, inducing mechanical effects such as microexplosions, displacement of absorbing structures (e.g., melanin granules), or hemorrhage (9–12). Such gross mechanical effects are often not tolerable in clinical applications. This paper discusses the concept of inducing tissue damage by repetitive short subthreshold pulses, each too small in energy to cause tissue damage by itself, in order to circumvent this limitation. Additivity has been demonstrated for multiple 40-μs pulses at 488 nm and 647 nm on the retina (13) and for multiple 9-ms CO_2 laser pulses on the cornea (14).

As an experimental model for such a selective damage mechanism, the rabbit retina has been chosen. The goal of this study was to destroy selectively the RPE cell monolayer by using multiple subthreshold effects with minimal damage to the directly adjacent photoreceptors in the neural retina.

The publication costs of this article were defrayed in part by page charge payment. This article must therefore be hereby marked "*advertisement*" in accordance with 18 U.S.C. §1734 solely to indicate this fact.

Concept

The transition from localized to more widespread thermal damage occurs as the exposure duration exceeds the thermal relaxation time (t_r) of the target structure. For a thermal point source $t_r = r^2/6k$, where k is the thermal diffusivity (1.5×10^{-3} $cm^2 s^{-1}$ for water) (1, 15). t_r is defined as the time at which the temperature at a point at distance r from the source has its maximum temperature. During exposure to long pulses ($p \gg t_r$), heat transfer occurs and the adjacent tissue is heated relatively uniformly, causing nonspecific necrosis.

If the pulse duration is well below the thermal relaxation time ($p \ll t_r$), spatial confinement can be achieved because the temperature rise outside the target structure of a chosen volume of radius r is too small to cause any significant collateral damage. For short pulses, however, high temperatures in the target structure are necessary to produce damage. When higher temperature gradients are induced, thermomechanical mechanisms such as explosive effects increasingly compete with pure thermally mediated ones.

We propose a concept based on the delivery of multiple short pulses. A specific combination of pulse duration, pulse energy, repetition rate, and number of pulses fractionally produces enough cumulative thermal load in the target structures to cause the desired tissue effect. Two assumptions are basic to the concept. (*i*) Each single pulse will induce a short, large temperature rise leading to thermal damage in the absorbing structure. The temperature decays quickly to almost body temperature during the interpulse time. Heat diffusion smooths out this strong temporal temperature modulation, and outside the absorbing volume a temperature increase with very limited modulation depth remains. If the relevant exposure parameters are chosen properly, the short strong temperature excursions in the target structure will cause an overall damage to the structure after application of a suitable number of subthreshold pulses. In contrast the small, smooth temperature rise in the surrounding tissue will not produce damage. (*ii*) Even though localized thermomechanical effects cannot be excluded, the thermal gradient induced by each single exposure stays below the threshold for undesirable gross mechanical damage.

Materials and Methods

An external acousto-optical modulator was used to chop a continuous-wave argon-ion laser beam (514 nm). The modulated argon laser beam was coupled to a laser slit lamp, which provided observation of the fundus and focusing of the laser beam onto the retina. The spot size at the neural retina was about 110 μm in diameter ($1/e^2$).

The retinas of Chinchilla rabbits were exposed to trains of short laser pulses or to single long exposures, longer than t_r

Abbreviation: RPE, retinal pigment epithelium.

‡To whom reprint requests should be addressed at the † address.

of the RPE. For short pulse exposure the pulse duration was always 5 μs. The pulse energy was varied in the range of 2, 3, 6, and 10 μJ. Trains of 1, 25, 100, and 500 pulses were used. The repetition rate was 500 Hz. The exposure times of the long control pulses were 100 ms, 500 ms, and 1 s with powers between 5 and 50 mW.

Animal care and anesthesia were in accordance with the institutional guidelines. A total of 800 short pulse exposures and 400 long pulse exposures in 40 eyes of 25 gray Chinchilla rabbits were performed. Both for short and for long pulses, the effect was assessed by fluorescein angiography about 2 hr and 1 day after exposure. Fluorescein, a fluorescent dye, leaks out of the choroid into the neural retina if the gap junctions between the RPE cells are broken. Fluorescein angiography is known as the most sensitive *in vivo* criterion for RPE alterations (16, 17). Statistical evaluation of all test exposures led to a quantitative definition of threshold parameters. Representative short- and long-pulse lesions were prepared for analysis by transmission electron microscopy (TEM) or light microscopy (LM) 2 hr and 1 day after exposure. Lesions at 2 hr: 20 pulsed lesions (100 pulses with each pulse 3 and 6 μJ; 500 pulses with each pulse 3 μJ and 6 μJ) were examined by TEM and LM; 16 continuous-wave lesions [10 of 50-ms exposure (35–45 mW)], 6 of 1-s exposure (10–16 mW) were examined by LM. Lesions at 1 day: 24 pulsed lesions (100 pulses of 3 μJ and 6 μJ) (20 by TEM and 4 by LM) and 24 continuous-wave lesions (20 by TEM and 4 by LM) were examined.

Results

Fig. 1 shows a probability plot of the lesions produced by repetitive short (5-μs) pulses. The incidence of damage visible by fluorescein angiography is plotted versus pulse energy for various numbers of pulses. The lines represent the linear regression curves. The threshold energy ED_{50} is the per-pulse energy necessary to achieve 50% probability of damage visible by fluorescein angiography. Fig. 1 indicates that ED_{50} decreases with increasing number of pulses, indicating some degree of additivity.

The results of the statistical evaluation of damage tests for single 1-s pulse exposures were analogously analyzed in a probit plot. The necessary power for 5% probability of fluorescein-visible RPE damage was 6 mW and that for 90% probability 17.5 mW. The threshold ED_{50} power at 1-s exposure time was ≈11 mW. The threshold powers for shorter continuous-wave exposure times were higher (e.g., 16.3 mW at 100-ms exposure times).

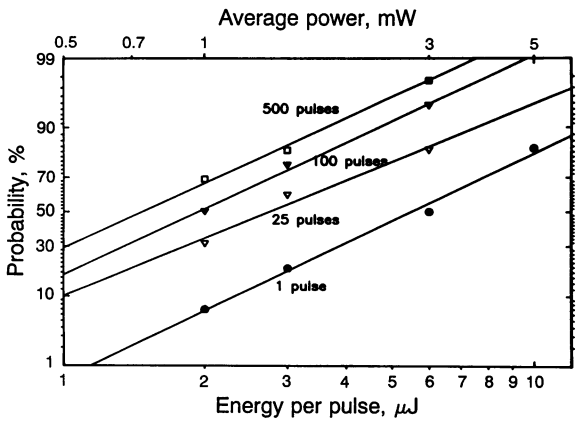

FIG. 1. Probability plot for a fluorescein angiographic visible damage in rabbit eyes after exposure to 1 (●), 25 (▽), 100 (▼), or 500 (□) short argon-laser pulses (514 nm) as a function of the energy per pulse at the cornea. Pulse duration, 5 μs; frequency, 500 Hz; laser spot diameter (*d*), 110 μm.

Histology of a typical lesion, irradiated with 500 short (5-μs) pulses at a frequency of 500 Hz (total exposure time, 1 s) is shown in Fig. 2. The pulse energy of 3 μJ was twice the ED_{50} value (Fig. 1). Histology of typical long pulse exposures (1 s with the ED_{50} power) is shown in Fig. 3. In both cases the target structure, the RPE, is heavily damaged with no recognizable cell processes left. The RPE shows disruption of individual cells, loss of cell membrane integrity, and condensation of cytoplasmic proteins. No cell borders can be seen. In both cases the melanin granules appear ultrastructurally normal and show no sign of displacement. Major differences appear in the damage of the directly adjacent tissues. After irradiation with repetitive short pulses the photoreceptor cells are aligned normally and most of them seem to be undamaged. The choriocapillaries are functionally patent and intact erythrocytes can be found. After long pulse irradiation all photoreceptor cells are uniformly destroyed. Erythrocytes in the choriocapillaries are clotted. Fig. 4 shows sections of lesions prepared 1 day after exposure to repetitive short laser pulses and after exposure to a single long (100-ms) continuous wave pulse. As in the sections prepared immediately after exposure, no outer segment damage is notable after exposure to repeated laser pulses. After a single 100-ms pulse with a power level only 20% above the angiographic threshold, all the outer and inner segments are damaged.

Thermal Modeling and Its Predictions

Light of 514 nm transmitted through the transparent medium and neural retina impinges on the RPE. A substantial amount of visible light is absorbed in the RPE (18, 19), directly adjacent to the neural retina. The RPE is a 10-μm thick monolayer of epithelial cells, heavily loaded with melanin granules, about 0.6 μm in diameter (20) as the only absorbers. In the rabbit RPE these granules are randomly distributed in the apical 4 μm of the RPE at an average spacing of about 1.2 μm (21).

Several thermal models have been developed to calculate the retinal temperature response due to laser exposure (1, 15, 22–25). In all these models, either the RPE is treated as a uniformly absorbing layer or the spacing of the granules is

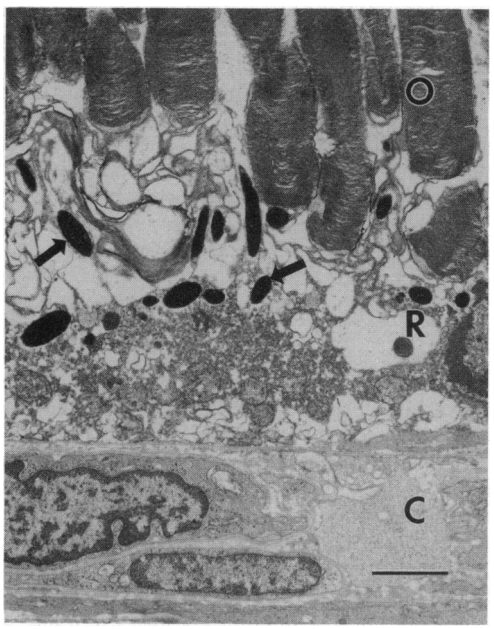

FIG. 2. Electron micrograph of a lesion 2 hr after exposure to 500 short pulses (5 μs, 500 Hz, 3 μJ, 514 nm, *d* = 110 mW), showing damage to the RPE (R) with sparing of the outer segments (O) of the photoreceptors and endothelium of the choriocapillaris (C). Melanin granules (arrows) appear ultrastructurally normal. (Bar = 2 μm.)

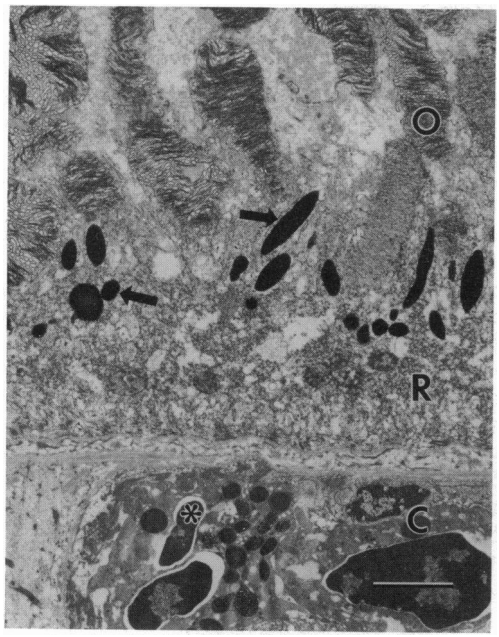

FIG. 3. Electron micrograph showing a lesion 2 hr after exposure to a long pulse (1 s, 10 mW, d = 110 μm). The RPE (R) and outer segments (O) of the photoreceptors show loss of cellular integrity. Note the endothelium in the choriocapillaris (C) is damaged and the presence of a leukocyte (asterisk). The damage to the RPE (R) is morphologically similar to the damage following pulsed irradiation. (Bar = 2 μm.)

assumed to be sufficiently wide so that the temperature at the boundary of one granule is independent of heat flow from neighboring granules (25). Both assumptions are not strictly valid and may lead to wrong results for short exposures. In this case the granularity of the absorber influences the microstructure of the temperature field. Two relaxation times (t_r) must be considered in the RPE. The t_r for a single granule is about 100 ns. The t_r for the heat flow out of the melanin-loaded 4-μm-thick homogeneous apical part of the RPE is about 5 μs.

The calculations of the model presented here are based on a homogeneous distribution of granules at an average distance of 1.2 μm. Each melanin granule was modeled as a cylinder with a radius of 0.3 μm and a length of 0.6 μm, oriented along the laser beam axis. A uniform distribution of 6620 continuous point sources of equal strength (26) was used to calculate the temperature profile inside and outside the melanin granule. Each point source releases heat at a prescribed rate. The numerical error of the solution in the center of a melanin granule, where an analytical solution is available, is <2% (15).

The solution for the spatial and temporal temperature variation, $T(r, t)$, after exposure to N_{max} pulses is obtained as the linear superposition of the contribution from i point sources to

$$T(r, t) = \frac{Q}{4\pi\lambda} \sum_{i=1}^{\infty} \frac{1}{r_i} \sum_{n=1}^{N_{max}} \left[\operatorname{erfc}\left(\frac{r_i}{\{4k[t - (n-1)\Delta t]\}^{1/2}} \right) - \operatorname{erfc}\left(\frac{r_i}{\{4k[t - (n-1)\Delta t - p]\}^{1/2}} \right) \right],$$

where k is thermal diffusivity ($m^2 \cdot s^{-1}$), λ is thermal conductivity ($W \cdot K^{-1} \cdot m^{-1}$), p is exposure time (s), Δt is the period of pulsing (1/frequency) (s), n is the pulse number, r_i is the distance to point source i (m), Q is power ($J \cdot s^{-1}$), and t is time (s). The fraction of the incident laser light (514 nm) that is absorbed by a single melanin granule was assumed to be 63%,

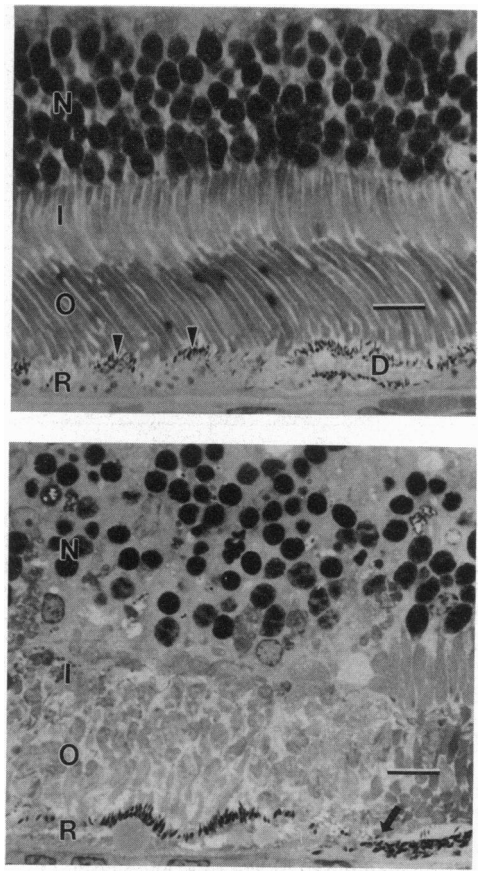

FIG. 4. (*Upper*) Light micrograph taken 24 hr after irradiation with repetitive pulsed laser (100 pulses, 6 μJ, 500 Hz, d = 110 μm). The retina shows little damage. RPE cells have covered Bruch's membrane under debris (D), which remains in the subretinal space. Note hypertrophic RPE cells (arrowhead). N, outer nuclear layer; I, inner segments; O, outer segments; R, RPE. (Bar = 10 μm.) (*Lower*) Light micrograph taken 24 hr after 100 ms of continuous irradiation (20 mW, d = 110 μm). The retina remains severely damaged. Most nuclei are pyknotic; outer segments (O), inner segments (I), and RPE (R) are damaged. Adjacent RPE shows a cytoplasmic extension under the debris (arrow). (Bar = 10 μm.)

which is in accord with the experimentally measured total absorption in the RPE of about 50% at 514 nm (18, 19). Shielding effects and light scattering in the RPE were neglected. Thermal properties of water were assumed (ρ = 1 $g \cdot cm^{-3}$, c = 4.19 $J \cdot g^{-1} \cdot K^{-1}$, a = 1.5 × 10^{-3} $cm^2 \cdot s^{-1}$). A Gaussian laser-beam profile with a diameter d ($1/e^2$) of 110 μm was used. The transmission from the cornea to the RPE was taken to be 93% (1).

The model has been tested by comparing its solutions with those of a homogeneous single-layer model (1), which is also experimentally well tested (21). For long pulse exposures the two models yield exactly the same results.

For pulse durations approaching the t_r for the RPE, the differences between a homogeneous layer model and a discrete absorber model become increasingly more pronounced. The temperature modulation in space between single melanin granules inside the RPE starts to appear as the pulse duration approaches t_r. In Fig. 5 the axial temperature profile at the center of the laser beam across the thickness of the RPE and into the neural retina is plotted for a single 5-μs exposure of 5.5-μJ pulse energy (ED_{50} threshold energy for a single 5-μs pulse) and for a 1-s pulse exposure of 11-mW (ED_{50} threshold power) for various times after exposure. A sharp temperature gradient at the border between the RPE and neural retina can be seen after a 5-μs pulse, in contrast to the gradient after the

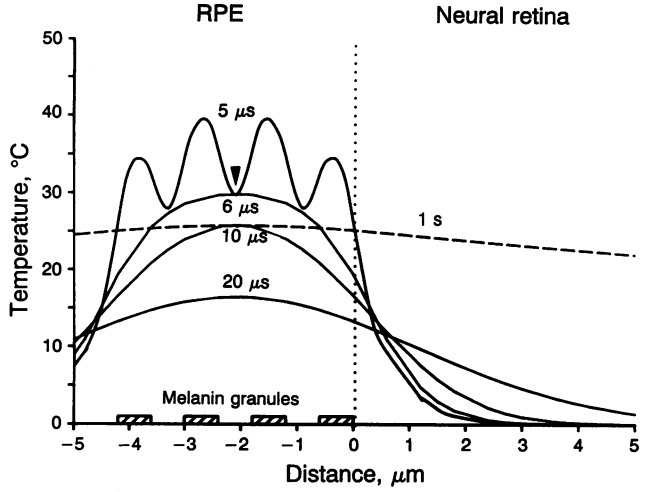

FIG. 5. Spatial temperature profile of the RPE and the neural retina in the laser beam axis after irradiation with a 5.5-μJ short (5-μs) laser pulse (threshold of single pulse). Dashed line shows the temperature profile after a long (1-s) pulse at threshold power (11 mW). Arrowhead indicates the location of the "reference point" as described in the text. A sharp temperature gradient is observed at the end of a short pulse. The short-pulse temperature profile is repetitively built up every 2 ms.

1-s exposure. This gradient is not significantly different for a 1-s and a 100-ms exposure (data not shown). In Fig. 6 the temperature time dependence at the reference point inside the RPE (arrowhead in Fig. 5) is plotted. At the end of a 5-μs pulse a maximum temperature increase of 5.5°C/μJ of pulse energy can be calculated at the reference point (Fig. 5). Fig. 6 shows the corresponding temperature time dependence in the neural retina 5 μm away from the RPE. The temporal temperature modulation at the reference point in the RPE is roughly 10 times that in the neural retina, only 5 μm away from the RPE. The average temperatures at the two sites (Fig. 6, smooth lines in RPE and neural retina) differ by only 20%, however. Nowhere does the difference exceed 7°C.

In contrast, for long pulse exposures of 100-ms, 500-ms, and 1-s duration and ED_{50} power the maximum temperatures at the reference point inside the RPE (reached at the end of the exposures) are calculated to be 35°C, 29°C, and 25°C, respectively.

Discussion

The morphological results clearly show the fundamental differences between the two photocoagulation concepts. The effects in the target structure, the RPE, morphologically look very similar. The striking difference is the damage to the adjacent structures. The results show that there is some additivity of the light-induced effects for repetitive laser pulses. The relationship between the number of pulses delivered (N) and the per-pulse energy (E_N) necessary to produce angiographically visible damage of the RPE is roughly $E_N/E_S = N^{-1/4}$ where E_S is the threshold energy for a single pulse exposure of equal damage. This is in agreement with other studies (13, 14, 27).

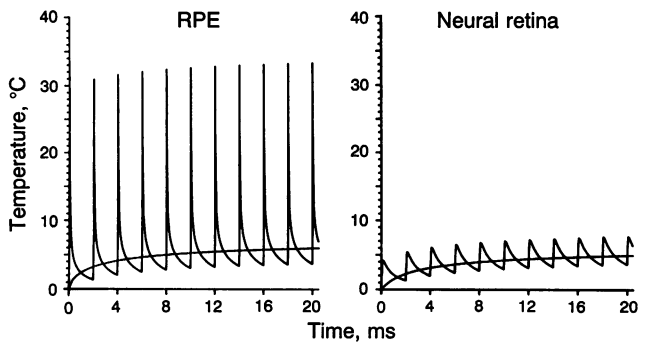

FIG. 6. Temperature time course in the RPE (between two melanin granules) and in the neural retina exposed to irradiation with repetitive short pulses of argon laser light (5 μs, 500 Hz, 5.5 μJ, 514 nm, d = 110 μm). In the target structure (RPE) the temperature increase is about 10 times higher than in the adjacent structure (neural retina).

The effects cannot be attributed to the average power of the pulse train, since the average power of the pulsed irradiation was only 1–5 mW. At these average power levels irradiation with long pulses did not produce a fluorescein-angiographically visible damage to the RPE, even for a 1-s exposure time. The total exposure time of the pulse train (2.5 ms, 3 mJ) seems unlikely to have caused the damage. The exposure time is about 500 times the thermal relaxation time. With 3-ms exposure times to 3 mJ from an argon laser and 500 μm spot sizes, the histological appearance is similar to that following conventional, continuous-wave photocoagulation, and either no blanching or hemorrhage is observed (28). In our experiments neither blanching nor bleeding has been observed. The energy differences for single long exposures and for repetitively short pulsed exposures also do not support a photochemical mechanism (29). Typical signs of acoustomechanical damage—e.g., bleeding, disruption of granules, displacement of melanin granules—were not observed in our study (Fig. 2). On the contrary, they have been found at energy densities typically 2–4 orders of magnitude above the 20–100 mJ/cm² used by us (10–12).

These findings strongly support the notion that thermal interaction mechanisms are mainly responsible for the RPE damage. With repetitively applied short laser pulses the adjacent structure, the neural retina, is spared because of the sharp temperature gradient at the border between RPE and retina. Each laser pulse leads to a short temperature increase in the target structure, the RPE. Before the next laser pulse is delivered, heat dissipates and the RPE has cooled to about 10% of the peak temperature (°C). The heat dissipation out of the RPE after each laser pulse leads to only a nonsignificant average temperature increase of <0.9°C/μJ of pulse energy inside the adjacent structure, the neural retina (5 μm from the RPE). This means that for the extreme case of 500 laser pulses of 5.5-μJ energy each, the peak temperature 5 μm from the RPE increases by <7°C. The average temperature rise at steady state, reached after roughly 5 pulses, is even smaller (about 5°C). As the long-pulse-exposure experiments show, RPE and neural retina damage occurs at a much greater temperature increase, about 25°C for a 1-s exposure.

The findings reported here suggest that the RPE damage observable after the train of repetitive 5-μs pulses is dominated by the temperature peaks inside the RPE. Highest temperatures occur inside the melanin granules. For threshold exposure with a single 5-μs pulse the temperature increase in a melanin granule can be calculated to be 40°C, only 5°C above the temperature increase of a 100-ms threshold exposure. This is a surprisingly small temperature difference considering the difference in time duration and assuming a first-order rate process for thermal damage. If more pulses are delivered less energy per pulse is necessary. This results in an even lower peak temperature. If, for example, 500 pulses at threshold are applied (time of pulse train, 1 s) the peak temperature increase inside the melanin granules is about 12.5°C, compared with that necessary for a continuous temperature rise (about 25°C) generated by a 1-s threshold exposure. Both irradiation modalities, however, produce the same morphological effect. A consistent first-order rate process model for damage (1, 2, 7) would require a temperature

rise in the melanin granules during pulsed irradiation much in excess of that needed for continuous irradiation.

This disagreement with the generally assumed thermal denaturation kinetics could mean that the damage mechanism is in reality not purely thermal but partly supported by thermomechanical effects. Such mechanical damage should have a very limited subcellar damage range and may not be detectable by electron microscopy. Such effects could include, for example, microvibrations of the melanin granules or increased pressure in the immediate neighborhood of the granules.

For short pulse durations, however, predictions of the peak temperature inside the melanin granules depend strongly on the actual geometry and the thermal properties of the granules. Such microstructure effects are negligible as long as the pulse duration exceeds the thermal relaxation time by several orders of magnitude and heat diffusion is dominating. For computational reasons our model is based on a cylindrical geometry of melanin granules. A spherical geometry leads to about 20% higher increase in temperatures (°C) in the center of the granules (15). In addition our model assumes that the granules have the thermal properties of water. The knowledge of thermal properties of natural melanin is incomplete (30). The heat capacity per unit volume for melanin is supposed to be smaller than that of water [3.44 $J \cdot K^{-1} \cdot cm^{-3}$ (31); 3.82 $J \cdot K^{-1} \cdot cm^{-3}$ (32)], whereas the thermal conductivity (6.3×10^{-3} $J \cdot cm^{-1} \cdot K^{-1} \cdot s^{-1}$) and the thermal diffusivity (1.65×10^{-3} $cm^2 \cdot s^{-1}$) are similar to the values for water (32). A smaller heat capacity of melanin again results in higher peak temperatures. Biophysical implications of thermal properties and absorption coefficients changing gradually during exposures are not counted in our model but could be important in repetitive photocoagulation. The absorption coefficient of synthetic melanin is strongly dependent on the redox potential and on the pH (32). All these uncertainties could result in higher peak temperatures inside the melanin granule.

Experiments performed on the microvasculature of hamster cheek pouches, where the occlusion of vessels with a single pulse and 100 short pulses (each 160 μs) were studied (33), support the generality of the concept reported here.

We have demonstrated the concept of *in vivo* selective photocoagulation by repetitive pulsed exposure in retinal structures, where we were able to damage a monocellular layer. The concept should be applicable to several other clinically interesting target tissues, such as the microvasculature, pigmented skin lesions, and, possibly, structures as small as single cells and molecules to which suitable chromophores have been linked.

We gratefully acknowledge helpful discussions with Rox Anderson. Norman Michaud provided the histological observations. This work was supported in part by the Office of Naval Research and Medical Free Electron Laser program under contract N0014-86-K-0117 and by the Deutsche Forschungsgemeinschaft, Bonn, Germany (Ro 804/1-1).

1. Birngruber, R., Hillenkamp, F. & Gabel, V.-P. (1985) *Health Phys.* **48** (6), 781–796.
2. Moussa, N. A., McGrath, J. J., Cravalho, E. G. & Asimacopoulos, P. J. (1977) *J. Biomech. Eng.* **99**, 155–159.
3. Bresnick, G. H. (1983) *Ophthalmology* **90**, 1301–1317.
4. Wallow, I. H. (1984) *Arch. Ophthalmol.* **102**, 126–135.
5. Tso, M. O., Cunha-Vaz, J. G., Shih, C. & Jones, C. W. (1980) *Arch. Ophthalmol.* **98**, 2032–2040.
6. Anderson, R. & Parrish, J. A. (1983) *Science* **220**, 524–527.
7. Arrhenius, S. (1889) *Z. Phys. Chem.* **4**, 226–248.
8. Henriques, F. C. (1947) *Arch. Pathol.* **43**, 489–502.
9. Cleary, S. F. (1977) in *Laser Applications in Medicine and Biology*, ed. Wolbarsht, M. L. (Plenum, London), Vol. 3, pp. 175–220.
10. Marshall, J. (1970) *Invest. Ophthalmol.* **9**, 97–115.
11. Marshall, J. & Mellerio, J. (1968) *Exp. Eye Res.* **7**, 225–230.
12. Zysset, B., Fujimoto, J., Puliafito, C. A., Birngruber, R. & Deutsch, T. F. (1989) *Lasers Surg. Med.* **9**, 193–204.
13. Ham, W. T., Mueller, H. A., Wolbarsht, M. L. & Sliney, D. H. (1988) *Health Phys.* **54**, 337–344.
14. Bargeron, C. B., Deters, O. J., Farrel, R. A. & McCally, R. L. (1989) *Health Phys.* **56** (1), 85–95.
15. Vassiliadis, A. (1971) in *Medicine and Biology*, ed. Wolbarsht, M. L. (Plenum, London), Vol. 1, pp. 125–162.
16. Birngruber, R., Puliafito, C. A., Gawande, A., Wei-Zhu, L., Schoenlein, R. W. & Fujimoto, J. (1987) *IEEE J. Quantum Electron.* **10**, 1836–1844.
17. Borland, R. G., Brennan, D. H., Marshall, J. & Viveash, J. P. (1978) *Exp. Eye Res.* **27**, 471–493.
18. Gabel, V. P., Birngruber, R. & Hillenkamp, F. (1978) *Excerpta Med. Int. Congr. Ser. No. 450*, 658–662.
19. Geeraets, W. J., Williams, R. C., Chan, G., Ham, W. T., Jr., Du Pont, G. & Schmidt, H. (1962) *Invest. Ophthalmol.* **1**, 340–347.
20. Feeney, L., Grieshaber, J. H. & Hogan, M. J. (1965) in *Structure of the Eye*, ed. Rohen, J. W. (Schattauer, Stuttgart).
21. Birngruber, R., Gabel, V. P. & Hillenkamp, F. (1983) *Health Phys.* **44** (5), 519–531.
22. Gabay, S., Kremer, I., Ben-Sira, I. & Erez, G. (1988) *Lasers Surg. Med.* **8**, 418–427.
23. Mainster, M. A., White, T. J. & Wilson, P. W. (1970) *Bull. Math. Biophys.* **32**, 303–314.
24. Wissler, E. H. (1976) *IEEE Trans. Biomed. Eng.* **3**, 207–215.
25. Hansen, W. P. & Fine, S. (1968) *Applied Optics* **7** (1), 155–159.
26. Carslaw, H. S. & Jaeger, J. C. (1959) *Conduction of Heat in Solids* (Oxford Univ. Press, Oxford, U.K.).
27. Stuck, B. E., Lund, D. J. & Beatrice, E. S. (1978) *Institute Report No. 58* (Letterman Army Inst. Res., Div. Non-Ionizing Radiation, Dept. Biomed. Stress, Presidio of San Francisco, CA).
28. Birngruber, R., Gabel, V.-P. & Hillenkamp, F. (1977) in *Modern Problems in Ophthalmology*, ed. Streiff, E. B. (Karger, Basel), Vol. 18, pp. 383–390.
29. Parrish, J. A., Anderson, R. R., Urbach, F. & Pitts, D. (1978) *UV-A: Biological Effects of Ultraviolet Radiation with Emphasis on Human Responses to Long Wave Ultraviolet* (Plenum, New York), p. 112.
30. Kollias, N., Sayre, R. M., Zeise, L. & Chedekel, M. R. (1991) *J. Photochem. Photobiol. B* **9**, 135–160.
31. Hayes, J. R. & Wolbarsht, M. L. (1968) *Aerospace Med.* **39**, 474.
32. Grippa, P. R. & Viappiani, C. (1990) *Eur. J. Biophys.* **17**, 299–305.
33. Roider, J., Traccoli, J., Michaud, N., Flotte, T., Anderson, R. & Birngruber, R. (1992) *Invest. Ophthalmol. Vis. Sci.* **33/4**, 722.